4-2008

TRAIL mediates liver injury by the innate immune system in the bile duct-ligated mouse.

Alisan Kahraman
Mayo Clinic

Fernando J. Barreyro
Mayo Clinic

Steven F. Bronk
Mayo Clinic

Nathan W. Werneburg
Mayo Clinic

Justin L. Mott
University of Nebraska Medical Center, justin.mott@unmc.edu

See next page for additional authors

Published in final edited form as:
Hepatology. 2008 April ; 47(4): 1317–1330. doi:10.1002/hep.22136.

TRAIL Mediates Liver Injury by the Innate Immune System in the Bile Duct–Ligated Mouse

Alisan Kahraman[1,2], **Fernando J. Barreyro**[1], **Steven F. Bronk**[1], **Nathan W. Werneburg**[1], **Justin L. Mott**[1], **Yuko Akazawa**[1], **Howard C. Masuoka**[1], **Charles L. Howe**[3], and **Gregory J. Gores**[1]

1*Miles and Shirley Fitterman Center for Digestive Diseases, Division of Gastroenterology and Hepatology, Mayo Clinic, Rochester, MN*

2*Department of Gastroenterology and Hepatology, University Hospital Essen, Essen, Germany*

3*Department of Immunology, Mayo Clinic, Rochester, MN.*

Abstract

The contribution of tumor necrosis factor–related apoptosis-inducing ligand (TRAIL), a death ligand expressed by cells of the innate immune system, to cholestatic liver injury has not been explored. Our aim was to ascertain if TRAIL contributes to liver injury in the bile duct–ligated (BDL) mouse. C57/BL6 wild-type (wt), TRAIL heterozygote ($TRAIL^{+/-}$), and TRAIL knockout ($TRAIL^{-/-}$) mice were used for these studies. Liver injury and fibrosis were examined 7 and 14 days after BDL, respectively. Hepatic TRAIL messenger RNA(mRNA) was 6-fold greater in BDL animals versus sham-operated wt animals ($P < 0.01$). The increased hepatic TRAIL expression was accompanied by an increase in liver accumulation of natural killer 1.1 (NK 1.1)–positive NK and natural killer T (NKT) cells, the predominant cell types expressing TRAIL. Depletion of NK 1.1–positive cells reduced hepatic TRAIL mRNA expression and serum alanine aminotransferase (ALT) values. Consistent with a role for NK/NKT cells in this model of liver injury, stress ligands necessary for their recognition of target cells were also up-regulated in hepatocytes following BDL. Compared to sham-operated wt mice, BDL mice displayed a 13-fold increase in terminal deoxynucleotidyl transferase–mediated dUTP nick-end labeling (TUNEL) and an 11-fold increase in caspase 3/7–positive hepatocytes ($P < 0.01$). The number of TUNEL and caspase 3/7–positive cells was reduced by >80% in BDL TRAIL knockout animals ($P < 0.05$). Likewise, liver histology, number of bile infarcts, serum ALT values, hepatic fibrosis, and animal survival were also improved in BDL $TRAIL^{-/-}$ animals as compared to wt animals.

Conclusion—These observations support a pivotal role for TRAIL in cholestatic liver injury mediated by NK 1.1–positive NK/NKT cells.

Cholestasis, defined as an impairment in bile formation, is a common syndrome in clinical practice. For example, cholestasis is a prominent feature of biliary atresia, primary sclerosing cholangitis, primary biliary cirrhosis, and other forms of chronic biliary tract disease.[1–3] The retention of bile acids normally excreted into bile within the liver elicits a toxic response, especially hepatocyte injury. This cell-specific injury rapidly results in secondary activation of hepatic resident macrophages, Kupffer cells, and recruitment of other inflammatory cells into the liver, including neutrophils[4,5]; these cell types are all cellular components of the innate immune system.[6] This more generalized phase of injury by the innate immune system promotes

Address reprint requests to: Gregory J. Gores, M.D., Professor of Medicine, Mayo Clinic, 200 First Street SW, Rochester, MN 55905. E-mail: gores.gregory@mayo.edu; fax: 507-284-0762.

Potential conflict of interest: Nothing to report.

hepatic fibrosis, which leads to cirrhosis and sequelae of chronic liver failure. Currently, therapeutic options for the treatment of cholestatic liver injury are limited. Rational therapeutic strategies to reduce hepatic injury during cholestasis will be predicated upon a better understanding of the mechanisms of liver injury. Thus, further insight into the cellular mechanisms by which cholestasis causes hepatocyte injury is of biomedical and clinical importance.

Hepatocyte damage in human liver diseases commonly occurs by apoptosis.[7] Although apoptosis can be induced by a wide variety of stimuli and mechanisms, the hepatocyte is particularly susceptible to apoptosis by death receptors.[8] For example, mice deficient in Fas have reduced liver injury and hepatic fibrosis following bile duct ligation (BDL), a rodent model of cholestasis.[9,10] Bile acids also stimulate expression of another death receptor termed tumor necrosis factor–related apoptosis-inducing ligand receptor 2 (TRAIL-R2), which is also called death receptor 5 (DR5).[11] When engaged by its cognate ligand tumor necrosis factor–related apoptosis-inducing ligand (TRAIL), this receptor also induces apoptosis by mechanisms analogous to Fas signaling.[12] Although TRAIL is not thought to induce cell death of normal hepatocytes, it does cause apoptosis of virally infected, transformed cells and fatty acid–treated hepatocytes.[13–16] More importantly, TRAIL has been shown to potentiate cytotoxic Fas signaling in the liver.[17] TRAIL enhances Fas-mediated hepatotoxicity by inducing sustained activation of c-Jun-N-terminal kinase (JNK), a member of the mitogen-activated protein kinase family that contributes to many forms of liver injury.[18] Thus, TRAIL activation synergistically augments Fas-mediated hepatotoxicity, a mechanism of liver injury potentially relevant to cholestatic liver damage. Despite this potential synergistic toxicity, the role of TRAIL in cholestatic liver injury has not been explored.

The ligands for death receptors are expressed predominantly by cells of the innate and adaptive immune system. Indeed, TRAIL itself is expressed by cells of the innate immune system, especially natural killer (NK) cells, natural killer T (NKT) cells, and monocytes.[19] We have previously examined TRAIL expression by Kupffer cells in the BDL mouse liver.[20] TRAIL expression by Kupffer cells was minimal as compared to their expression of the other death ligands, tumor necrosis factor α and Fas ligand. However, TRAIL expression by NK/NKT cells and the contribution of these cell types to liver injury in this model have not been explored. Given the importance of NK/NKT cells in other forms of liver injury, their potential contribution to hepatocyte apoptosis, liver injury, and fibrosis warrants further study.[21] If NK cells are to contribute to cholestatic liver injury of hepatocytes, they would need a recognition system. NK cells recognize target cells, in part, by the cytotoxic natural killer group 2 member D receptor, which binds glycoprotein stress ligands.[22] The murine stress ligands include H60, murine UL16-binding protein-like transcript 1 (MULT-1), and retinoic acid early inducible gene 1α (RAE-1α), RAE-1β, RAE-1γ, RAE-1δ, and RAE-1ε.[22] Of these stress ligands, H60 is the most abundantly expressed in many forms of injury.[23]

The overall objective of this study was to determine if NK/NKT cells contribute to liver injury by a TRAIL-dependent mechanism. To address this subject, we examined the role of NK/NKT cells in cholestatic liver injury and employed BDL wild-type (wt), TRAIL heterozygote ($TRAIL^{+/-}$), and TRAIL homozygote ($TRAIL^{-/-}$) mice. The results of this study support a critical role for TRAIL in cholestatic liver injury by the innate immune system.

Materials and Methods

Animal Models

The care and use of the animals for these studies were reviewed and approved by the Institutional Animal Care and Use Committee at the Mayo Clinic. C57/BL6 wt, $TRAIL^{+/-}$, and $TRAIL^{-/-}$ mice (6–8 weeks of age, 20–25 g body weight) were employed for these studies.

The TRAIL$^{+/-}$ and TRAIL$^{-/-}$ mice were obtained from Taconic Farm, Inc. (Hudson, NY) via an agreement with Amgen, Inc. (Thousand Oaks, CA).[24,25] Mice were maintained in a temperature-controlled (22°C), pathogen-free environment and fed a standard rodent chow diet and water ad libitum. For experimental procedures, mice were anesthetized with ketamine (60 mg/kg of body weight) plus xylazine (10 mg/kg of body weight) by intraperitoneal injection. After a midline upper-abdominal incision, the peritoneal cavity was opened, the abdominal wall was retracted, and the common hepatic bile duct was double-ligated and divided between the ligatures as previously described by us in detail.[9] Sham-operated wt mice, used as controls, under-went laparotomy with exposure but no ligation of the common bile duct. The fascia and skin of the midline abdominal incision were closed with sterile surgical 5–0 sutures (ETHICON, Inc., Somerville, NJ). After 3, 7, or 14 days of BDL, depending on the experimental procedures, mice were reanesthetized, and blood was obtained from the vena cava inferior for serum alanine aminotransferase (ALT), total bilirubin, and bile acid (total bile acid colorimetric assay kit, Bio-Quant, Inc., San Diego, CA) determinations[26] prior to liver tissue being procured for additional studies (vide infra). As both NK and NKT cells express the cell marker NK 1.1, we will refer to these cell populations collectively as NK 1.1–positive NK/NKT cells. To investigate the role of hepatic NK 1.1–positive NK/NKT cells and TRAIL during cholestasis, wt mice were bile duct–ligated for 7 days with or without the depletion of NK 1.1–positive cells by intraperitoneal injection of either a specific anti-NK 1.1 monoclonal antibody (PK 136, BD Bioscience, San Jose, CA; 250 μg on days −1, 3, and 7 post-BDL) or a nonspecific immunoglobulin G (IgG) isotype–matched monoclonal antibody (JIE7-c, Developmental Studies Hybridoma Bank, University of Iowa) under similar conditions.[27] In all models of liver injury, the liver was removed and cut into small pieces and either snap-frozen in liquid nitrogen for storage at −80°C or fixed in freshly prepared 4% paraformaldehyde in phosphate-buffered saline for 24 hours at 4°C. Liver sections were also subjected to RNA extraction using the TRIzol reagent (Invitrogen, Carlsbad, CA).

Histopathology

For histological review of hematoxylin and eosin (H&E)–stained liver sections by light microscopy (Eclipse Meta Morph V 5.0.7, Nikon, West Lafayette, IN), the liver was diced into 5 mm × 5 mm sections, fixed in 4% paraformaldehyde for 48 hours, and then embedded in paraffin. Tissue sections (4 μm) were prepared using a microtome (Reichert Scientific Instruments, Buffalo, NY) and placed on glass slides. H&E staining was performed according to standard techniques.

Terminal Deoxynucleotidyl Transferase–Mediated dUTP Nick-End Labeling (TUNEL) Assay, Immunofluorescent Identification of Activated Caspases 3/7, and Cellular Colocalization of Cathepsin B and Lysosome-Associated Membrane Protein 1 (LAMP-1)

Apoptotic cells were quantitated by the TUNEL assay, which enzymatically labels free 3′-OH ends of damaged DNA with a fiuorescently labeled nucleotide as we have previously described in detail.[28] TUNEL-labeled cells (that is, fluorescent nuclei) were quantified by the number of positive cells per high-power field being counted. A total of 10 high-power fields were analyzed for each animal with excitation and emission wavelengths of 380 and 430 nm, respectively, using an inverted laser scanning confocal microscope (LSM 510, Carl Zeiss Micro-Imaging, Inc., Thornwood, NJ) equipped with a 40X NA 1.4 lens and LSM 510 imaging software. Data were expressed as the number of TUNEL-positive cells per 10 high-power fields. Immunofluorescence analysis for activated caspases 3/7 was performed using a rabbit anti-active caspase 3/7 polyclonal antibody (BD Biosciences/Pharmingen, San Diego, CA) recognizing a common neoepitope shared by activated caspases 3 and 7 as we have previously described.[28] The liver specimens were viewed by confocal microscopy using excitation and emission wavelengths of 351 and 364 nm, respectively. The number of caspase 3/7–positive cells was quantified per 10 high-power fields as described above for the TUNEL assay.

Immunofluorescence analysis for cathepsin B was also performed as previously described by us.[29] Cellular localization of cathepsin B was demonstrated using colocalization with the lysosome marker LAMP-1 (H-228, Santa Cruz, Santa Cruz, CA). Liver specimens were viewed by confocal microscopy for cathepsin B (488 and 507 nm) and LAMP-1 (577 and 590 nm), respectively. Hepatocytes were scored according to their diffuse versus punctate fluorescent pattern per 10 high-power fields. Data were expressed as percent diffuse of total hepatocytes scored. Negative control slides were incubated with non-immune immunoglobulin for both the caspase 3/7 and cathepsin B/LAMP-1 immunohistochemistry.

Identification of Hepatic NK and NKT Cells by Immunohistochemistry

The tissue sections were pre-incubated with Block-ace (Dako Cytomation, Inc., Carpinteria, CA) for 10 minutes at 37°C to block nonspecific binding of the primary antibody. Endogenous peroxidise activity was blocked with 0.3% H_2O_2 and 0.1% NaN_3 in distilled water for 10 minutes at room temperature. The sections were then incubated with 1:500 diluted biotin-conjugated anti-NK 1.1 mouse primary antibody (BD Bioscience) overnight, rinsed three times with phosphate-buffered saline, and then incubated with avidin-biotin peroxidase complexes (Vector Laboratories, Burlingame, CA). Histochemical development was achieved with a commercial 3,3′-diaminobenzidine (DAB) substrate kit (Vector Laboratories). Finally, the sections were counterstained for 3 minutes with hematoxylin and coverslipped with mounting medium for light microscopy.

Isolation of Mouse Hepatocytes

Mouse hepatocytes were isolated by collagenase perfusion through the hepatic portal vein as described previously.[30] Mouse hepatocytes were purified by Percoll gradient centrifugation[31]; average viability by trypan blue exclusion was 90%.

Quantitative Real Time–Polymerase Chain Reaction (rt-PCR)

Total RNA was isolated from liver tissue using the TRIzol Reagent (Invitrogen). For each RNA sample, a 10-μg aliquot was reverse-transcribed into complementary DNA (cDNA) using an oligo-dT random primer and Maloney murine leukemia virus reverse transcriptase (Invitrogen) as previously described in detail.[32] After the reverse transcription reaction, the cDNA template was amplified by rt-PCR with Taq DNA polymerase (Invitrogen) using standard protocols. All amplified polymerase chain reaction (PCR) products were confirmed by electrophoresis in 1% low–melting temperature agarose gel, stained with ethidium bromide, and photographed using ultraviolet illumination. The expected base pair (bp) PCR products were identified, and the bands were cut from the gel. Next, PCR products were eluted into trishydroxymethylaminomethane (Tris)-HCl using a DNA elution kit (Qiagen, Valencia, CA). The concentration of DNA in the extracted PCR product was measured spectrophotometrically (DU 4400, Beckman, Palo Alto, CA) as copies per milliliter at 260 nm. Extracted PCR products were prepared as standards at concentrations of 10^{10}, 10^9, 10^8, 10^7, 10^6, 10^5, 10^4, 10^3, and 10^2 copies/μL. For quantification studies, quantitative rt-PCR was performed using the Light Cycler (Roche Diagnostics Corp., Mannheim, Germany) and SYBR green as the fluorophore (Invitrogen). The inverse linear relationship between copy number and cycle number was then determined. This standard curve was used to calculate the copy number in the experimental sample. The copy number of messenger RNA (mRNA) in each sample was expressed as a relative ratio of product copies per milliliter to copies per milliliter of housekeeping gene 18S from the same RNA (respective cDNA) sample and PCR run.[11] PCR primers (all obtained from the Mayo DNA Synthesis Core Facility, Rochester, MN) were as follows: TRAIL-R2/DR5 forward 5′-TGA CGG GGA AGA GGA ACT GA-3′ and reverse 5′-GGC TTT GAC CAT TTG GAT TTG A-3′ (yielding a 389-bp product), TRAIL forward 5′-CCC TGC TTG CAG GTT AAG AG-3′ and reverse 5′-GGC CTA AGG TCT TTC CAT CC-3′ (yielding a 240-bp

product), α-smooth muscle actin (α-SMA) forward 5′-ACT ACT GCC GAG CGT GAG AT-3′ and reverse 5′-AAG GTA GAC AGC GAA GCC AG-3′ (yielding a 452-bp product), collagen 1α (I) forward 5′-GAA ACC CGAGGTATG CTT GA-3′ and reverse 5′-GAC CAG GAG GAC CAG GAA GT-3′ (yielding a 276-bp product), and finally NK 1.1 forward 5′-TCA TCC TCC TTG TCC TGA CC-3′ and reverse 5′-TTG AAT GAG CAG CAA AGT GG-3′ (yielding a 248-bp product). For quantitative rt-PCR of the stress ligands, the Light Cycler Taq Man Master kit and universal probes (Roche Diagnostics Corp., Indianapolis, IN) were used. Glyceraldehyde 3-phosphate dehydrogenase (GAPDH) primers were employed to normalize the samples. PCR primers, also obtained from the Mayo DNA Synthesis Core Facility, were as follows: GAPDH forward 5′-AGC TTG TCA TCA ACG GGA AG-3′ and reverse 5′-TTT GAT GTT AGT GGG GTC TCG-3′ (yielding a 240-bp product), H60 forward 5′-ACA GCA TAG CAT CTA CTT TTA TCC AC-3′ and reverse 5′-TCC ATG GCA CTG CTG TTA TC-3′ (yielding a 299-bp product), MULT-1 forward 5′-CAT GCC ATT GGT GCT CAT AG-3′ and reverse 5′-TGC TTG TGT CAA CAC GGA AT-3′ (yielding a 250-bp product), and finally pan-RAE-1 forward 5′-TGG ACA CTC ACA AGA CCA ATG-3′ and reverse 5′-CCC AGG TGG CAC TAG GAG T-3′ (yielding a 75-bp product).

Immunoblot Analysis

Liver tissue was directly lysed for 30 minutes on ice with a lysis buffer consisting of 50 mM/L Tris-HCl (pH 7.4), 1% Nonidet P-40, 0.25% sodium deoxycholate, 150 mM NaCl, 1 mM ethylene diamine tetraacetic acid, 1mM phenylmethylsulfonyl fluoride, 1 μg/mol aprotinin, 1 μg/mol leupeptin, 1 μg/mol pepstatin, 1 M Na_3VO_4, and 1 mM NaF. After centrifugation at 13,000*g* for 15 minutes at 4°C, the protein concentration in the supernatant was measured using Bradford's reagent (Bio-Rad, Hercules, CA). The supernatant protein was denatured by boiling for 10 minutes in distilled water. Protein (50 μg) was resolved by sodium dodecyl sulfate–polyacrylamide gel electrophoresis (SDSPAGE) on a gradient gel and then transferred onto nitrocellulose membranes. Blocking was carried out using 5% nonfat dairy milk in Tris-buffered saline (20 mM Tris, 150 mM NaCl, pH 7.4) with 0.1% Tween-20 for 1 hour at room temperature. Primary antibodies were diluted 1:1000 in a blocking solution and incubated overnight at 4°C. The following antibodies were used: anti-Bak (TC-102, mouse monoclonal antibody, Calbiochem, San Diego, CA), anti-FLIP (rabbit polyclonal IgG, Upstate Biotechnology, Lake Placid, NY), Bax (N-20, rabbit polyclonal IgG, Santa Cruz), Bcl-X_L (H-62, rabbit polyclonal IgG, Santa Cruz), Bid (M-20, goat polyclonal IgG, Santa Cruz), Bim (rat monoclonal antibody, Chemicon, Australia), Fas (X-20 G, goat polyclonal IgG, Santa Cruz), Fas-L (N-20, rabbit polyclonal antibody, Santa Cruz), Mcl-1 (rabbit anti-mouse Ab, Rockland, Gilbertsville, PA), and γ-Tubulin (mouse monoclonal antibody, Sigma-Aldrich Corp., St. Louis, MO). To detect antigenantibody complexes, peroxidise-conjugated secondary antibodies (Biosource International, Camarillo, CA) were diluted 1:3000 in a blocking solution and incubated for 45 minutes at room temperature. Immune complexes were visualized using chemiluminescent substrate (Amersham, IL) and Kodak X-OMAT film (Eastman Kodak, Rochester, NY) according to the manufacturer's instructions.

Immunohistochemistry for α-SMA and Determination of Liver Fibrosis by Sirius Red Staining

The sections were stained for α-SMA using amouse monoclonal antibody (NeoMarkers, Fremont, CA), which was prediluted in 0.05 mol/L Tris-HCl, pH 7.6, containing stabilizing protein and 0.015 mol/L sodium azide by the manufacturer for staining formalin-fixed, paraffin-embedded tissues. The sections were incubated with the primary antibody overnight at 4°C in a 1:200 dilution. Negative control slides were incubated with nonimmune immunoglobulin under the same conditions. Secondary reagents were obtained from the Dako Cytomation En Vision + System-HRP ready-to-use kit; DAB chromogen solution was used for visualization by light microscopy. Finally, the tissue was counterstained with hematoxylin for 3 minutes. Liver fibrosis was quantified using Sirius red staining as described by Arteel et

al.[33] Direct red 80 and Fast-green FCF (color index 42053) were obtained from Sigma-Aldrich Diagnostics. Liver sections were stained, and red-stained collagen fibers were quantified by digital image analysis as previously described by us in detail.[26]

Statistical Analysis

All data represent at least five separate experiments and are expressed as the mean ± standard error unless otherwise indicated. Differences between groups were compared using analysis of variance (ANOVA) for repeated measures and the post hoc Bonferroni test to correct for multiple comparisons. A *P* value less than 0.05 was considered to be statistically significant. All statistical analyses were performed using In-Stat Software (Graph Pad, San Diego, CA).

Results

Hepatic NK and NKT Cells Are Increased in the BDL Mouse and Contribute to Liver Injury

Initially, we sought to examine the role of NK/NKT cells in murine liver following BDL. To address this question, we performed immunohistochemistry for these cell types in the liver using antisera specific for the NK/NKT cell marker NK 1.1.[27] An increase in these cell types was observed in the BDL liver regardless of the mouse genotype—wt, $TRAIL^{+/-}$, or $TRAIL^{-/-}$ (Fig. 1A). Likewise, quantitative rt-PCR also demonstrated increased but similar mRNA expression levels for NK 1.1 in the liver of all three genotypes following BDL (Fig. 1B). In an additional study, wt mice following BDL for 7 days were treated either with a specific anti-NK 1.1 antibody or with a nonspecific, IgG isotype–specific, monoclonal antibody. As previously reported, [27] treatment of mice with the anti-NK 1.1 antibody, but not the nonspecific control antibody, markedly reduces the number ofNK1.1–positive cells in the liver (Fig. 1C). Consistent with the immunohistochemistry data, quantitative rt-PCR also demonstrated decreased mRNA expression levels for NK 1.1 in the livers of anti-NK 1.1–treated BDL wt mice versus control IgG-treated BDL wt mice (Fig. 1D). Histopathological examination of liver specimens from 7-day BDL wt mice demonstrated severe cholestatic hepatitis with widespread bile infarctions (confluent foci of feathery hepatocyte degeneration, a pathognomic feature of large bile duct obstruction; Fig. 2A), bile ductular proliferation, portal edema, and hepatocellular damage. Liver damage was markedly reduced in specimens from BDL wt animals upon treatment with the anti-NK 1.1 antibody. In addition, bile infarctions were also less evident in BDL wt mice treated with the anti-NK 1.1 antibody than in BDL wt mice treated with control, isotype-identical IgG (Fig. 2A). Determination of serum ALT values resulted in a significant decrease in BDL wt mice after depletion of NK 1.1–positive cells (Fig. 2B). NK 1.1–positive NK/NKT cells induce liver injury by recognition of stress ligands on target cells. [22] To further implicate these cells in liver injury following BDL, hepatic mRNA expression of the stress ligands—H60, MULT-1, and pan-RAE-1—was quantified in hepatocytes. Indeed, 4–6-, and 7-fold increases in expression of H60, MULT-1, and pan-RAE-1, respectively, were identified in hepatocytes of 3-day BDL wt mice versus sham-operated control mice (Fig. 3). Taken together, these observations demonstrate an increase in NK 1.1–positive NK/NKT cells as well as a preferential up-regulation of these stress ligands in the liver following BDL and implicate a role for these cells in this model of liver injury.

NK/NKT Cells Are the Predominant Source of TRAIL in the BDL Liver

Next, we ascertained if hepatic tissue TRAIL mRNA was increased following BDL. Indeed, after 7 days of BDL, a 6-fold significant increase in TRAIL mRNA was observed in wt animals as compared to sham-operated controls (6.8 ± 0.7 versus 1 ± 0.2 TRAIL/18S mRNA ratio, $P < 0.01$). Hepatic tissue TRAIL mRNA levels were significantly decreased in BDL wt mice after depletion of NK 1.1–positive cells (Fig. 4). These data indicate an increase in hepatic TRAIL expression due to an accumulation of NK 1.1–positive NK/ NKT cells in the BDL liver. However, this accumulation is not TRAIL-dependent.

Hepatocyte Apoptosis Is Reduced in the TRAIL-Deficient BDL Mouse

The above studies demonstrate that NK 1.1–positive NK/NKT cells contribute to cholestatic liver injury. Also, these cells are the source of increased TRAIL in the BDL liver. Next, we sought to determine if liver injury by these cells was TRAIL-dependent. Before embarking on a series of studies assessing apoptosis and liver injury in genetic models of BDL, we provided assurance that protein expression of apoptosis effectors was similar between both genotypes. Immunoblot analysis was performed for several apoptosis effector proteins including Fas, Bax, Bak, Bim, c-FLIP, Bid, Bcl-X_L, and Mcl-1 (Fig. 5A). Hepatic protein levels for these key apoptotic effectors were similar between wt and TRAIL-deficient mice under basal conditions. As TRAIL can enhance Fas-mediated hepatotoxicity and Fas plays a role in hepatic injury during BDL,[26] further immunoblot analyses for the Fas receptor and ligand were performed. As demonstrated (Fig. 5B), no alterations in the expression levels of the Fas receptor and ligand were observed in wt, TRAIL$^{+/-}$, and TRAIL$^{-/-}$ mice following BDL.

Next, to examine the effects of TRAIL in mediating hepatic apoptosis, wt, TRAIL$^{+/-}$, and TRAIL$^{-/-}$ mice were subjected to BDL for 7 days. Liver histopathology from wt animals demonstrated numerous clusters of apoptotic cells in a background of altered hepatic micro-architecture (Fig. 6A). Quantitation of these TUNEL-positive cells demonstrated a 13-fold increase in wt BDL mice compared to sham-operated controls. Consistent with an allelic dose effect, the number of TUNEL-positive cells observed in TRAIL$^{+/-}$ mice was intermediate between wt and TRAIL$^{-/-}$ BDL mice (Fig. 6A). The activation of executioner caspases, especially caspases 3 and 7, is a biochemical hallmark of apoptosis.[34] Therefore, to further confirm that hepatocyte apoptosis occurs in wt animals following BDL, we performed immunohistochemistry for activated caspases 3/7. Immunoreactive product was readily identified in liver tissues from wt mice following BDL but not in sham-operated controls (Fig. 6B). Consistent with the TUNEL assay, BDL wt animals demonstrated an 11-fold increase in the number of caspase 3/7–positive hepatocytes versus sham-operated controls (Fig. 6B). Caspase 3/7–positive cells were also reduced in TRAIL$^{-/-}$ BDL animals as compared to wt animals, with an intermediate number of positive cells in TRAIL$^{+/-}$ animals. Taken together, these data are consistent with TRAIL-potentiated apoptosis in BDL mice.

TRAIL Contributes to Liver Injury in the BDL Mouse

To determine if TRAIL-mediated hepatocyte apoptosis translates into significant hepatotoxicity, histopatho-logical examination of liver specimens was performed along with determination of serum ALT values. Histopathological examination of liver specimens from 7-day BDL wt mice displayed severe cholestatic hepatitis with widespread bile infarctions, bile ductular proliferation, portal edema, and hepatocellular damage. Liver damage was reduced in specimens from TRAIL$^{+/-}$ and TRAIL$^{-/-}$ animals following 7 days of BDL (Fig. 7A). In addition, bile infarctions were also less evident in BDL TRAIL$^{+/-}$ and TRAIL$^{-/-}$ mice (Fig. 7B). A marked reduction in serum ALT values in TRAIL$^{+/-}$ and TRAIL$^{-/-}$ animals as compared to wt mice was also observed 7 days following BDL (Fig. 7C). Differences in hepatocyte apoptosis and liver injury could not be ascribed to alterations in cholestasis because total bilirubin determinations (Fig. 7D) as well as total bile acid concentrations (Fig. 7E) in BDL mice were almost identical, indicating similar cholestatic effects of BDL between groups of animals. The decrease in liver injury in the TRAIL$^{-/-}$ mice was due to a reduction in hepatocyte apoptosis. Thus, these data suggest that the death ligand TRAIL is hepatotoxic in animals with obstructive cholestasis.

TRAIL Cytotoxicity Is Associated with Lysosomal Release of Cathepsin B

We have recently reported that TRAIL cytotoxicity in cultured human hepatoma cell lines is associated with a redistribution of cathepsin B from lysosomes into the cytosol.[35] To ascertain if this also occurs in vivo following BDL, liver sections were examined by coimmuno

fluorescence for cathepsin B and LAMP-1 (a lysosomal-associated membrane protein and a marker for lysosomes). Under basal conditions in sham-operated controls, cells displayed a punctate pattern for cathepsin B and LAMP-1 consistent with lysosomal cathepsin B localization. However, following 7 days of BDL, hepatocytes of wt mice revealed a diffuse fluorescence pattern for cathepsin B suggesting a redistribution of cathepsin B from lysosomes into the cytosol, whereas the fluorescence pattern for LAMP-1 remained punctate (Fig. 8A). In contrast, cells from BDL TRAIL$^{+/-}$ and TRAIL$^{-/-}$ animals displayed a mixed fluorescence pattern for cathepsin B, with the majority of cells examined displaying a punctate pattern of fluorescence (Fig. 8A). The percentage of cells with a diffuse distribution of cathepsin B was increased in wt mice as compared to TRAIL$^{+/-}$ and TRAIL$^{-/-}$ BDL mice (Fig. 8B). These data demonstrate that following BDL, cathepsin B undergoes a cellular redistribution from lysosomes into the cytosol by a TRAIL-dependent process.

Markers of Hepatic Fibrogenesis Are Diminished in TRAIL$^{-/-}$ Animals Following BDL for 14 Days

If the reduction of liver injury in TRAIL$^{-/-}$ mice is significant, it should also translate into reduced hepatic fibrosis, a sequela of liver damage. Because stellate cells are the principal hepatic cell type responsible for collagen deposition in the liver,[36] we next quantified transcripts for stellate cell activation by rt-PCR. After 14 days of BDL, mRNA for α-SMA, a cardinal marker for stellate cell activation, was increased 11-fold in wt mice as compared to sham-operated mice. More importantly, the transcript for α-SMA was reduced in TRAIL$^{-/-}$ animals (Fig. 9A). Consistent with the mRNA data, α-SMA immunoreactivity was also increased in the sinusoids of BDL wt mice but reduced in BDL TRAIL$^{+/-}$ mice (Fig. 9B). To ascertain if stellate cell activation was also associated with enhanced hepatic fibrogenesis, mRNA for hepatic collagen 1α (I) was quantified. Collagen 1α (I) mRNA expression was increased 3-fold in wt mice versus TRAIL$^{-/-}$ mice after BDL (Fig. 9C). Hepatic collagen protein deposition was identified in liver specimens by Sirius red staining (Fig. 9D) and subjected to quantitative morphometry.[26] Collagen staining by Sirius red was increased 4-fold in wt BDL mice versus TRAIL$^{-/-}$ BDL mice (Fig. 9D). Collectively, these data suggest that in wt animals following BDL for 14 days, hepatic stellate cell activation and hepatic fibrogenesis are attenuated in TRAIL$^{-/-}$ mice, likely secondary to the reduced liver injury in these animals.

Survival of TRAIL$^{-/-}$ Animals Is Enhanced Following BDL

Given that liver injury and fibrogenesis are significantly reduced in TRAIL$^{-/-}$ animals, we reasoned that animal survival should also be enhanced. Therefore, in our final series of studies, we examined overall animal survival in BDL mice. By day 14 after BDL, 80% of TRAIL$^{-/-}$ animals were still alive compared to only 20% in the wt animal group (Fig. 10). Taken together, these studies demonstrate that during cholestasis, deficiency of TRAIL exerts an important prosurvival effect. Given that the TRAIL deletion is not liver-specific, the organ-specific effects responsible for enhanced animal survival cannot be specifically delineated. However, as germ line TRAIL deletion reduces liver injury, hepato-protection likely, in part, contributes to the improved animal survival.

Discussion

Cholestatic liver injury is an exceedingly complex pathophysiologic syndrome. We have previously implicated a role for the innate immune system in cholestatic liver injury by Kupffer cells.[20] The current study extends these observations by elucidating a role for NK/NKT cells in this process. NK/NKT cell–dependent liver injury was TRAIL-dependent. Enhanced TRAIL expression is a special feature of hepatic NK cells due to their unique responsiveness to interleukin-2 as compared to peripheral NK cells.[19] Although NK cells can induce cell death

by both perforin/granzyme B–dependent and TRAIL-dependent mechanisms,[37] hepatocytes richly express the granzyme B inhibitors, proteinase inhibitor 9 and serine proteinase inhibitor 6, which limit injury by the perforin/granzyme B mechanism.[38] Therefore, our results demonstrating TRAIL-dependent and NK/NKT cell–dependent liver injury in the BDL murine liver are consistent with the current concepts regarding NK cells in liver pathobiology. These data are also consistent with the emerging concept that the liver is an integral organ of the innate immune system[39,40] and is often activated with deleterious consequences during pathophysiologic disturbances.

Unexpectedly, we observed an accumulation of fat in the livers of wt BDL mice after depletion of NK cells (Fig. 1C). Prior studies have shown, however, that in genetically obese, leptin-deficient mice, hepatic NK cells are depleted. This cellular depletion was associated with steatohepatitis, reduced hepatic expression of anti-inflammatory cytokines, and increased activity of pro-inflammatory cytokines.[41,42] The steatosis observed by depletion of NK 1.1–positive NK/NKT cells in our study is therefore consistent with previous studies suggesting that this cellular population negatively regulates neutral fat deposition in hepatocytes. It is very unlikely that fat could be an explanation for the resistance of the BDL to TRAIL-mediated injury as fat actually sensitizes hepatocytes to TRAIL.[16,43]

Genetic deletion of TRAIL reduced hepatocyte apoptosis in the BDL mouse. Although TRAIL is nontoxic to normal hepatocytes,[44] it is cytotoxic to transformed,[45] virally infected,[46] free fatty acid–treated,[16,43] and bile acid–treated hepatocytes.[11] Therefore, TRAIL can directly induce hepatocyte cytotoxicity in disease states. During cholestasis, hepatocytes are likely sensitized to TRAIL because of bile acid–mediated up-regulation of the cognate receptor TRAIL-receptor 2.[11,47] TRAIL's cytotoxic effect in cholestasis could also be by an indirect rather than direct mechanism. TRAIL can potentiate Fas-induced liver injury by activating JNK,[17] and Fas deletion also reduces hepatic injury and fibrosis in the BDL mouse.[26] Taken together, these observations suggest potential cooperativity between the two death receptors in the BDL mouse. This cooperativity is especially likely as NK cells express both Fas ligand and TRAIL[48] and likely engage their respective receptors on the target hepatocyte membrane. Whether its cytotoxicity is direct or indirect, TRAIL appears to play an integral role in cholestatic liver injury.

We have previously implicated cathepsin B as a mediator of liver injury and fibrogenesis in the BDL mouse.[49] Indeed, mice genetically deficient for cathepsin B have reduced liver injury and fibrosis. However, in those studies, neither the release of cathepsin B from lysosomes into the cytosol nor the mechanisms for lysosomal permeabilization were examined. The current studies, therefore, extend the prior observations by demonstrating a redistribution of cathepsin B from a lysosomal compartment into the cytosol of hepatocytes following BDL. This phenomenon was absent in TRAIL-deficient BDL mice, and this observation is consistent with TRAIL-mediated lysosomal permeabilization in vitro.[35] Given that Fas stimulation does not induce permeabilization of liver lysosomes,[50] release of cathepsin B from lysosomes into the cytosol appears to be TRAIL-mediated.

We and others have previously suggested that TRAIL is cytotoxic for activated stellate cells.[51,52] Solely on the basis of these observations, genetic deletion of TRAIL would have been predicted to enhance hepatic fibrosis. In contrast, we observed reduced hepatic fibrosis in $TRAIL^{-/-}$ BDL mice. The reduced hepatic fibrosis is best explained by the observed reduction in hepatocyte apoptosis in TRAIL-deficient mice. Hepatic fibrogenesis is mediated by activated stellate cells, which are the principal source of collagen I in the liver. Apoptosis can activate this cell type by two recognized mechanisms involving phagocytosis of apoptotic bodies. These remnants of the apoptotic process can be phagocytosed by Kupffer and/or stellate cells.[4,20] This phagocytotic process activates both cell types. Kupffer cell engulfment of

apoptotic bodies results in expression of transforming growth factor β, a profibrogenic cytokine that activates stellate cells by a paracrine mechanism.[36] Alternatively, phagocytosis of apoptotic bodies directly by stellate cells also results in their expression of transforming growth factor β, which, in a cell autonomous manner, may drive activation by an autocrine process.[53] Either cellular mechanism could account for the reduction of hepatic fibrosis by apoptosis inhibition in the current study.

In summary, TRAIL deletion attenuates liver injury and improves animal survival in the BDL mouse. These data are consistent with a critical role for TRAIL as a mediator of hepatic damage during cholestasis in preclinical models. Mechanisms to disrupt TRAIL signaling pathways, such as modulating NK/NKT cell activation, could prove to be therapeutic in human cholestatic liver diseases. These data also suggest TRAIL agonists should be used with caution during cholestasis, as TRAIL may prove to be hepatotoxic in this syndrome.

Abbreviations

α-SMA, α-smooth muscle actin
ALT, alanine aminotransferase
ANOVA, analysis of variance
BDL, bile duct ligation/bile duct–ligated
bp, base pair
cDNA, complementary DNA
DAB, 3,3'-diaminobenzidine
DR5, death receptor 5
GAPDH, glyceraldehyde 3-phosphate dehydrogenase
H&E, hematoxylin and eosin
hpf, high-power field
IgG, immunoglobulin G
JNK, c-Jun-N-terminal kinase
LAMP, lysosome-associated membrane protein
mRNA, messenger RNA
MULT-1, murine UL16-binding protein-like transcript 1
NK, natural killer
NKT, natural killer T
PCR, polymerase chain reaction
RAE-1, retinoic acid early inducible gene 1
rt-PCR, real time–polymerase chain reaction
SDS-PAGE, sodium dodecyl sulfate–polyacrylamide gel electrophoresis
TRAIL, tumor necrosis factor–related apoptosis-inducing ligand
$TRAIL^{-/-}$, TRAIL homozygote
$TRAIL^{+/-}$, TRAIL heterozygote
TRAIL-R2, tumor necrosis factor–related apoptosis-inducing ligand receptor 2
Tris, trishydroxymethylaminomethane
TUNEL, terminal deoxynucleotidyl transferase–mediated dUTP nick-end labeling
wt, wild-type

Acknowledgment

The authors thank Erin Bungum for her excellent secretarial assistance, James Tarara from the Division of Biochemistry and Molecular Biology (Mayo Clinic, Rochester, MN) for quantitation of the Sirius red images, Jason G. Kerkvliet and Reghann G. LaFrance from the Department of Immunology (Mayo Clinic) for technical assistance with the rt-PCR of the stress ligands, and the anonymous reviewers for their most valuable and insightful suggestions.

Supported by a fellowship grant from the Association for Scientific Research and Science at the Department of Gastroenterology and Hepatology, University Hospital Essen, Duisburg-Essen University (Essen, Germany) to A.K., by grant DK 41876 from the National Institutes of Health to G.J.G., and by the Mayo Foundation (Rochester, MN).

References

1. Emerick KM, Whitington PF. Neonatal liver disease. Pediatr Ann 2006;35:280–286. [PubMed: 16637557]
2. LaRusso NF, Shneider BL, Black D, Gores GJ, James SP, Doo E, et al. Primary sclerosing cholangitis: summary of a workshop. HEPATOLOGY 2006;44:746–764. [PubMed: 16941705]
3. Lazaridis KN, Talwalkar JA. Clinical epidemiology of primary biliary cirrhosis: incidence, prevalence, and impact of therapy. J Clin Gastroenterol 2007;41:494–500. [PubMed: 17450033]
4. Canbay A, Taimr P, Torok N, Higuchi H, Friedman S, Gores GJ. Apoptotic body engulfment by a human stellate cell line is profibrogenic. Lab Invest 2003;83:655–663. [PubMed: 12746475]
5. Gujral JS, Farhood A, Bajt ML, Jaeschke H. Neutrophils aggravate acute liver injury during obstructive cholestasis in bile duct-ligated mice. HEPATOLOGY 2003;38:355–363. [PubMed: 12883479]
6. Racanelli V, Rehermann B. The liver as an immunological organ. HEPATOLOGY 2006;43:S54–S62. [PubMed: 16447271]
7. Rust C, Gores GJ. Apoptosis and liver disease. Am J Med 2000;108:567–574. [PubMed: 10806286]
8. Yoon JH, Gores GJ. Death receptor-mediated apoptosis and the liver. J Hepatol 2002;37:400–410. [PubMed: 12175638]
9. Miyoshi H, Rust C, Roberts PJ, Burgart LJ, Gores GJ. Hepatocyte apoptosis after bile duct ligation in the mouse involves Fas. Gastroenterology 1999;117:669–677. [PubMed: 10464144]
10. Gujral JS, Liu J, Farhood A, Jaeschke H. Reduced oncotic necrosis in Fas receptor-deficient C57BL/6J-lpr mice after bile duct ligation. HEPATOLOGY 2004;40:998–1007. [PubMed: 15382126]
11. Higuchi H, Bronk SF, Takikawa Y, Werneburg N, Takimoto R, El-Deiry W, et al. The bile acid glycochenodeoxycholate induces trail-receptor 2/DR5 expression and apoptosis. J Biol Chem 2001;276:38610–38618. [PubMed: 11507096]
12. Sheridan JP, Marsters SA, Pitti RM, Gurney A, Skubatch M, Baldwin D, et al. Control of TRAIL-induced apoptosis by a family of signaling and decoy receptors. Science 1997;277:818–821. [PubMed: 9242611]
13. Ashkenazi A, Pai RC, Fong S, Leung S, Lawrence DA, Marsters SA, et al. Safety and antitumor activity of recombinant soluble Apo2 ligand. J Clin Invest 1999;104:155–162. [PubMed: 10411544]
14. Walczak H, Miller RE, Ariail K, Gliniak B, Griffith TS, Kubin M, et al. Tumoricidal activity of tumor necrosis factor-related apoptosis-inducing ligand in vivo. Nat Med 1999;5:157–163. [PubMed: 9930862]
15. Sadarangani A, Kato S, Espinoza N, Lange S, Llados C, Espinosa M, et al. TRAIL mediates apoptosis in cancerous but not normal primary cultured cells of the human reproductive tract. Apoptosis 2007;12:73–85. [PubMed: 17136491]
16. Malhi H, Barreyro F, Isomoto H, Bronk SF, Gores GJ. Free fatty acids sensitize hepatocytes to trial medicated cytotoxicity. Gut 2007;56:1124–1131. [PubMed: 17470478]
17. Corazza N, Jakob S, Schaer C, Frese S, Keogh A, Stroka D, et al. TRAIL receptor-mediated JNK activation and Bim phosphorylation critically regulate Fas-mediated liver damage and lethality. J Clin Invest 2006;116:2493–2499. [PubMed: 16955144]
18. Jones BE, Czaja MJ III. Intracellular signaling in response to toxic liver injury. Am J Physiol 1998;275:G874–G878. [PubMed: 9815013]
19. Herr I, Schemmer P, Buchler MW. On the TRAIL to therapeutic intervention in liver disease. HEPATOLOGY 2007;46:266–274. [PubMed: 17596886]
20. Canbay A, Feldstein AE, Higuchi H, Werneburg N, Grambihler A, Bronk SF, et al. Kupffer cell engulfment of apoptotic bodies stimulates death ligand and cytokine expression. HEPATOLOGY 2003;38:1188–1198. [PubMed: 14578857]
21. Jeong WI, Park O, Radaeva S, Gao B. STAT1 inhibits liver fibrosis in mice by inhibiting stellate cell proliferation and stimulating NK cell cytotoxicity. HEPATOLOGY 2006;44:1441–1451. [PubMed: 17133483]

22. Lanier LL. NK cell recognition. Annu Rev Immunol 2005;23:225–274. [PubMed: 15771571]
23. Radaev S, Sun PD. Structure and function of natural killer cell surface receptors. Annu Rev Biophys Biomol Struct 2003;32:93–114. [PubMed: 12471063]
24. Ashkenazi A. Targeting death and decoy receptors of the tumour-necrosis factor superfamily. Nat Rev Cancer 2002;2:420–430. [PubMed: 12189384]
25. Kelley RF, Totpal K, Lindstrom SH, Mathieu M, Billeci K, Deforge L, et al. Receptor-selective mutants of apoptosis-inducing ligand 2/tumor necrosis factor-related apoptosis-inducing ligand reveal a greater contribution of death receptor (DR) 5 than DR4 to apoptosis signaling. J Biol Chem 2005;280:2205–2212. [PubMed: 15520016]
26. Canbay A, Higuchi H, Bronk SF, Taniai M, Sebo TJ, Gores GJ. Fas enhances fibrogenesis in the bile duct ligated mouse: a link between apoptosis and fibrosis. Gastroenterology 2002;123:1323–1330. [PubMed: 12360492]
27. Liu ZX, Govindarajan S, Kaplowitz N. Innate immune system plays a critical role in determining the progression and severity of acetaminophen hepatotoxicity. Gastroenterology 2004;127:1760–1774. [PubMed: 15578514]
28. Natori S, Selzner M, Valentino KL, Fritz LC, Srinivasan A, Clavien PA, et al. Apoptosis of sinusoidal endothelial cells occurs during liver preservation injury by a caspase-dependent mechanism. Transplantation 1999;68:89–96. [PubMed: 10428274]
29. Baskin-Bey ES, Canbay A, Bronk SF, Werneburg N, Guicciardi ME, Nyberg SL, et al. Cathepsin B inactivation attenuates hepatocyte apoptosis and liver damage in steatotic livers after cold ischemia-warm reperfusion injury. Am J Physiol Gastrointest Liver Physiol 2005;288:G396–G402. [PubMed: 15472011]
30. Klaunig JE, Goldblatt PJ, Hinton DE, Lipsky MM, Chacko J, Trump BF. Mouse liver cell culture. I. Hepatocyte isolation. In Vitro 1981;17:913–925. [PubMed: 6273298]
31. Seglen PO. Preparation of isolated rat liver cells. Methods Cell Biol 1976;13:29–83. [PubMed: 177845]
32. Kurosawa H, Que FG, Roberts LR, Fesmier PJ, Gores GJ. Hepatocytes in the bile duct-ligated rat express Bcl-2. Am J Physiol 1997;272:G1587–G1593. [PubMed: 9227497]
33. Arteel GE, Raleigh JA, Bradford BU, Thurman RG. Acute alcohol produces hypoxia directly in rat liver tissue in vivo: role of Kupffer cells. Am J Physiol 1996;271:G494–G500. [PubMed: 8843775]
34. Cohen GM. Caspases: the executioners of apoptosis. Biochem J 1997;326(pt 1):1–16. [PubMed: 9337844]
35. Guicciardi ME, Bronk SF, Werneburg NW, Gores GJ. cFLIPL prevents TRAIL-induced apoptosis of hepatocellular carcinoma cells by inhibiting the lysosomal pathway of apoptosis. Am J Physiol Gastrointest Liver Physiol 2007;292:G1337–G1346. [PubMed: 17272514]
36. Reeves HL, Friedman SL. Activation of hepatic stellate cells—a key issue in liver fibrosis. Front Biosci 2002;7:D808–D826. [PubMed: 11897564]
37. van Dommelen SL, Sumaria N, Schreiber RD, Scalzo AA, Smyth MJ, Degli-Esposti MA. Perforin and granzymes have distinct roles in defensive immunity and immunopathology. Immunity 2006;25:835–848. [PubMed: 17088087]
38. Barrie MB, Stout HW, Abougergi MS, Miller BC, Thiele DL. Antiviral cytokines induce hepatic expression of the granzyme B inhibitors, proteinase inhibitor 9 and serine proteinase inhibitor 6. J Immunol 2004;172:6453–6459. [PubMed: 15128837]
39. John B, Crispe IN. TLR-4 regulates CD8+ T cell trapping in the liver. J Immunol 2005;175:1643–1650. [PubMed: 16034104]
40. Hotamisligil GS. Inflammation and metabolic disorders. Nature 2006;444:860–867. [PubMed: 17167474]
41. Guebre-Xabier M, Yang S, Lin HZ, Schwenk R, Krzych U, Diehl AM. Altered hepatic lymphocyte subpopulations in obesity-related murine fatty livers: potential mechanism for sensitization to liver damage. HEPATOLOGY 2000;31:633–640. [PubMed: 10706553]
42. Li Z, Soloski MJ, Diehl AM. Dietary factors alter hepatic innate immune system in mice with nonalcoholic fatty liver disease. HEPATOLOGY 2005;42:880–885. [PubMed: 16175608]

43. Volkmann X, Fischer U, Bahr MJ, Ott M, Lehner F, Macfarlane M, et al. Increased hepatotoxicity of tumor necrosis factor-related apop tosis-inducingligand in diseased human liver. HEPATOLOGY 2007;46:1498–1508. [PubMed: 17705261]
44. Ichikawa K, Liu W, Zhao L, Wang Z, Liu D, Ohtsuka T, et al. Tumoricidal activity of a novel anti-human DR5 monoclonal antibody without hepatocyte cytotoxicity. Nat Med 2001;7:954–960. [PubMed: 11479629]
45. Koschny R, Walczak H, Ganten TM. The promise of TRAIL-potential and risks of a novel anticancer therapy. J Mol Med. 2007
46. Afford SC, Adams DH. Following the TRAIL from hepatitis C virus and alcohol to fatty liver. Gut 2005;54:1518–1520. [PubMed: 16227354]
47. Higuchi H, Bronk SF, Taniai M, Canbay A, Gores GJ. Cholestasis increases tumor necrosis factor-related apoptosis-inducing ligand (TRAIL)-R2/DR5 expression and sensitizes the liver to TRAIL-mediated cytotoxicity. J Pharmacol Exp Ther 2002;303:461–467. [PubMed: 12388624]
48. Smyth MJ, Hayakawa Y, Takeda K, Yagita H. New aspects of natural killer-cell surveillance and therapy of cancer. Nat Rev Cancer 2002;2:850–861. [PubMed: 12415255]
49. Guicciardi ME, Deussing J, Miyoshi H, Bronk SF, Svingen PA, Peters C, et al. Cathepsin B contributes to TNF-alpha-mediated hepatocyte apoptosis by promoting mitochondrial release of cytochrome c. J Clin Invest 2000;106:1127–1137. [PubMed: 11067865]
50. Wattiaux R, Wattiaux-de Coninck S, Thirion J, Gasingirwa MC, Jadot M. Lysosomes and Fas-mediated liver cell death. Biochem J 2007;403:89–95. [PubMed: 17129211]
51. Taimr P, Higuchi H, Kocova E, Rippe RA, Friedman S, Gores GJ. Activated stellate cells express the TRAIL receptor-2/death receptor-5 and undergo TRAIL-mediated apoptosis. HEPATOLOGY 2003;37:87–95. [PubMed: 12500193]
52. Radaeva S, Sun R, Jaruga B, Nguyen VT, Tian Z, Gao B. Natural killer cells ameliorate liver fibrosis by killing activated stellate cells in NKG2D dependent and tumor necrosis factor-related apoptosis-inducing ligand dependent manners. Gastroenterology 2006;130:435–452. [PubMed: 16472598]
53. Canbay A, Friedman S, Gores GJ. Apoptosis: the nexus of liver injury and fibrosis. HEPATOLOGY 2004;39:273–278. [PubMed: 14767974]

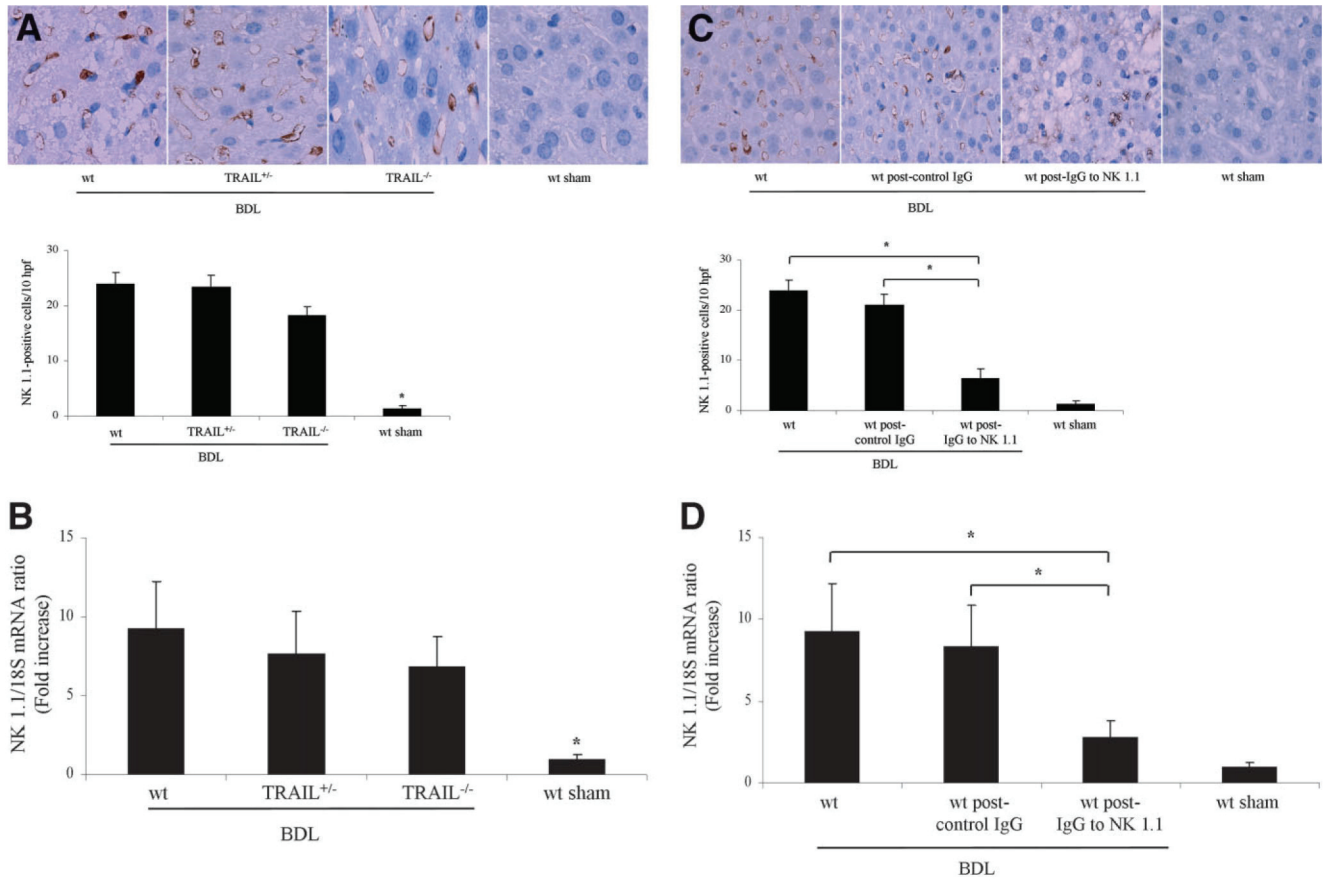

Fig. 1.

Hepatic NK 1.1–positive cells are increased following BDL. (A) Immunohistochemistry for NK 1.1 cells demonstrated an almost identical increase of NK 1.1–positive cells in the BDL livers of wt, TRAIL$^{+/-}$, and TRAIL$^{-/-}$ animals (magnification by light microscopy 60X). Quantitation of NK 1.1–positive cells demonstrated a significant increase in BDL mice as compared to sham-operated mice. *$P < 0.01$ by ANOVA. Data from five independent animals per group are expressed as the mean ± standard error. (B) Quantitative rt-PCR demonstrated almost equal mRNA expression levels for NK 1.1 in the livers of all three genotypes following BDL. *$P < 0.01$ by ANOVA for BDL mice versus sham-operated wt mice. (C) Immunohistochemistry for NK 1.1 cells demonstrated an almost identical increase of these cell types in wt and IgG-treated wt animals following BDL. wt mice following BDL and NK cell depletion displayed fewer hepatic NK cells along with accumulation of fat in the liver. Quantitation of NK 1.1 cells demonstrated a significant decrease in BDL wt mice after NK cell depletion as compared to BDL wt mice treated with control, isotype-identical IgG. Data from five independent animals per group are expressed as the mean ± standard error. *$P < 0.05$ by ANOVA. (D) Quantitative rt-PCR demonstrated decreased mRNA expression levels for NK 1.1 cells in the livers of NK cell-depleted wt mice as compared to control IgG-treated wt mice following BDL.

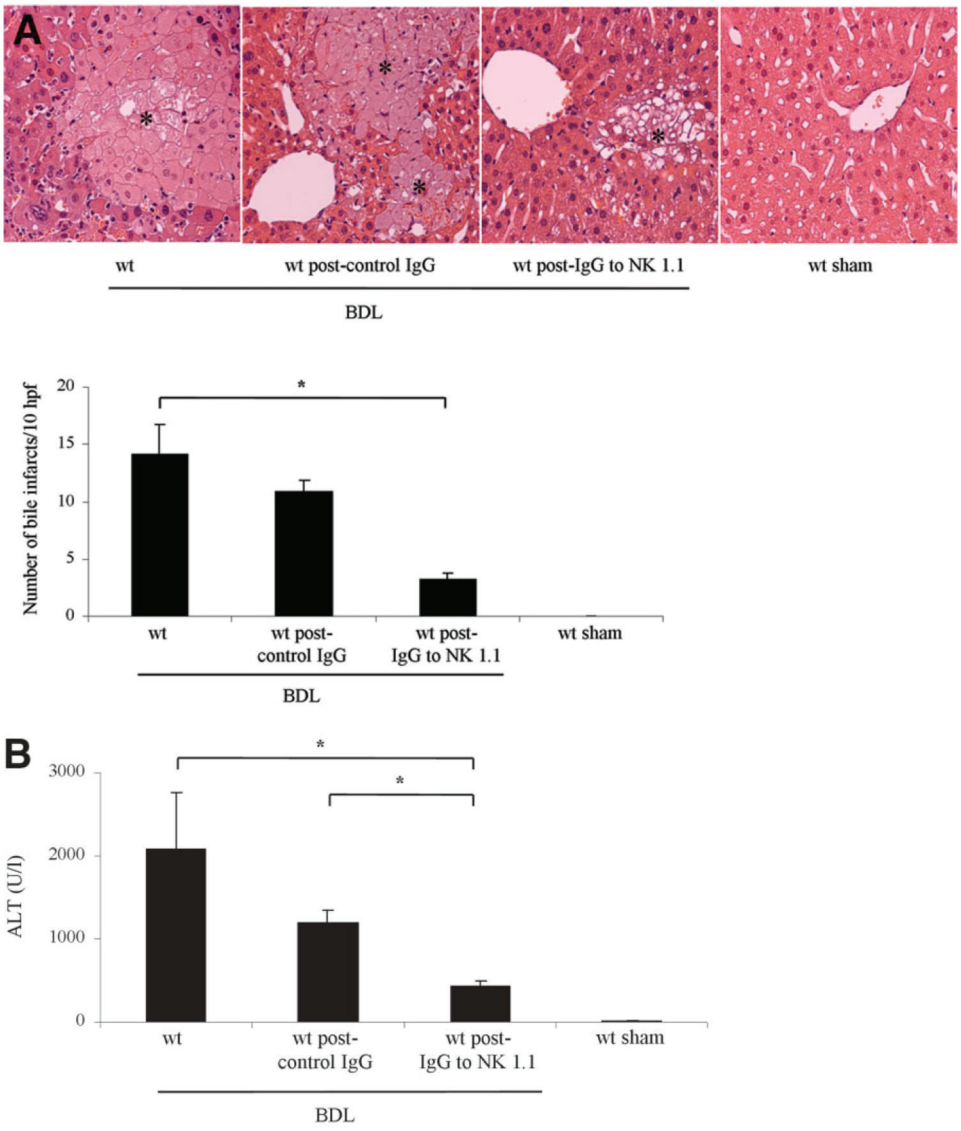

Fig. 2.

Liver injury in the BDL mouse is NK/NKT cell-dependent. Representative photomicrographs of conventional H&E-stained liver sections (magnification 40X) are shown. (A) Liver specimens of wt BDL mice displayed significant and extensive hepatocyte injury with bile infarcts (marked with asterisks), bile duct proliferation, and portal edema. BDL-induced liver injury was reduced in wt animals upon treatment with the anti-NK 1.1 antibody and was absent in liver sections of sham-operated control mice. Bile infarcts (confluent foci of hepatocyte feathery degeneration caused by bile acid cytotoxicity) were quantified and were also less evident in BDL wt mice treated with the anti-NK 1.1 antibody. (B) Serum ALT values were measured 7 days after BDL and demonstrated a significant decrease in BDL wt mice after depletion of NK 1.1–positive cells from the liver. Data are from five independent animals and are expressed as the mean ± standard error. *$P < 0.05$ by ANOVA.

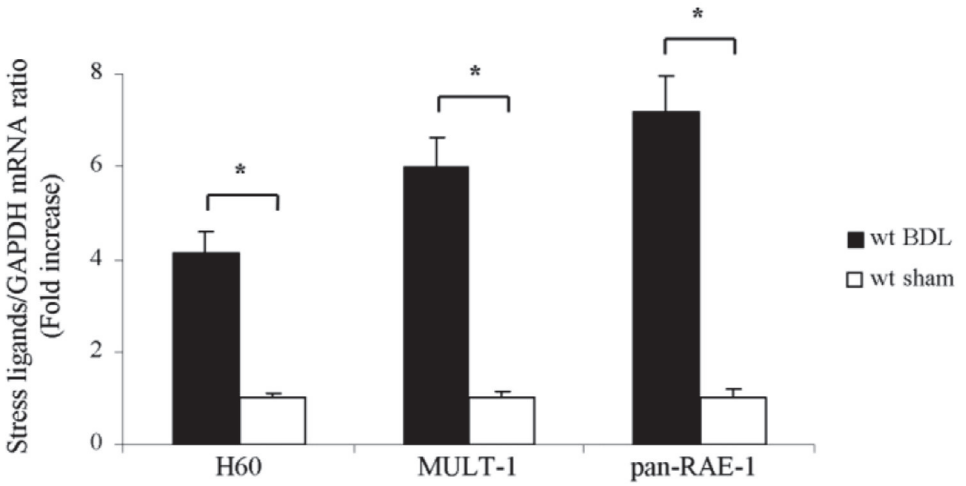

Fig. 3.

Hepatocytes up-regulate stress ligands following BDL. Quantitative rt-PCR demonstrated increased hepatic mRNA expression levels of the stress ligands H60, MULT-1, and pan-RAE-1 in hepatocytes of 3-day BDL wt mice versus sham-operated control mice. Data are from five independent animals and are expressed as the mean ± standard error. **P* < 0.05 by ANOVA.

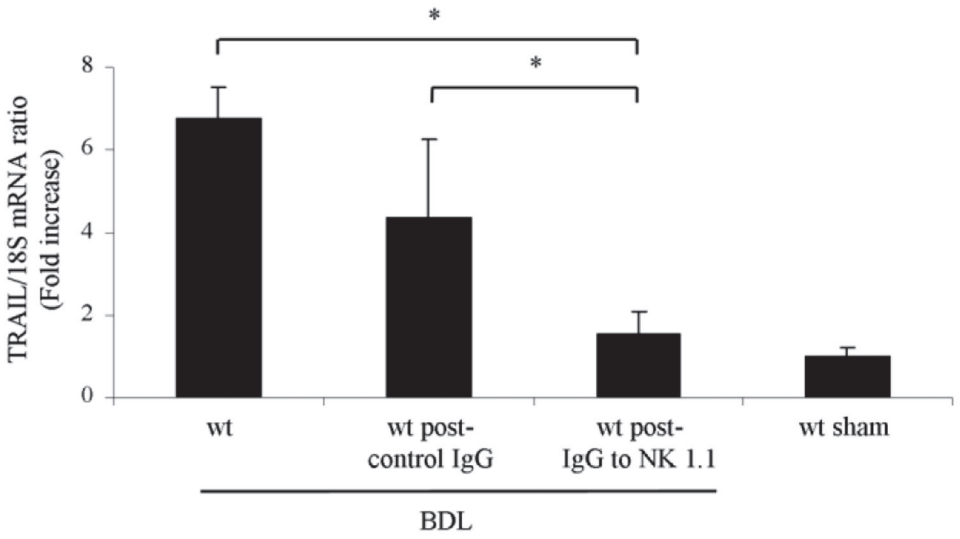

Fig. 4.

NK/NKT cells are the predominant source of increased TRAIL in the BDL liver. Quantitative rt-PCR demonstrated decreased mRNA expression levels for TRAIL in the livers of BDL wt mice after depletion of NK 1.1–positive cells. Data points represent experiments from five independent animals, and bars are expressed as the mean ± standard error. *$P < 0.05$ by ANOVA.

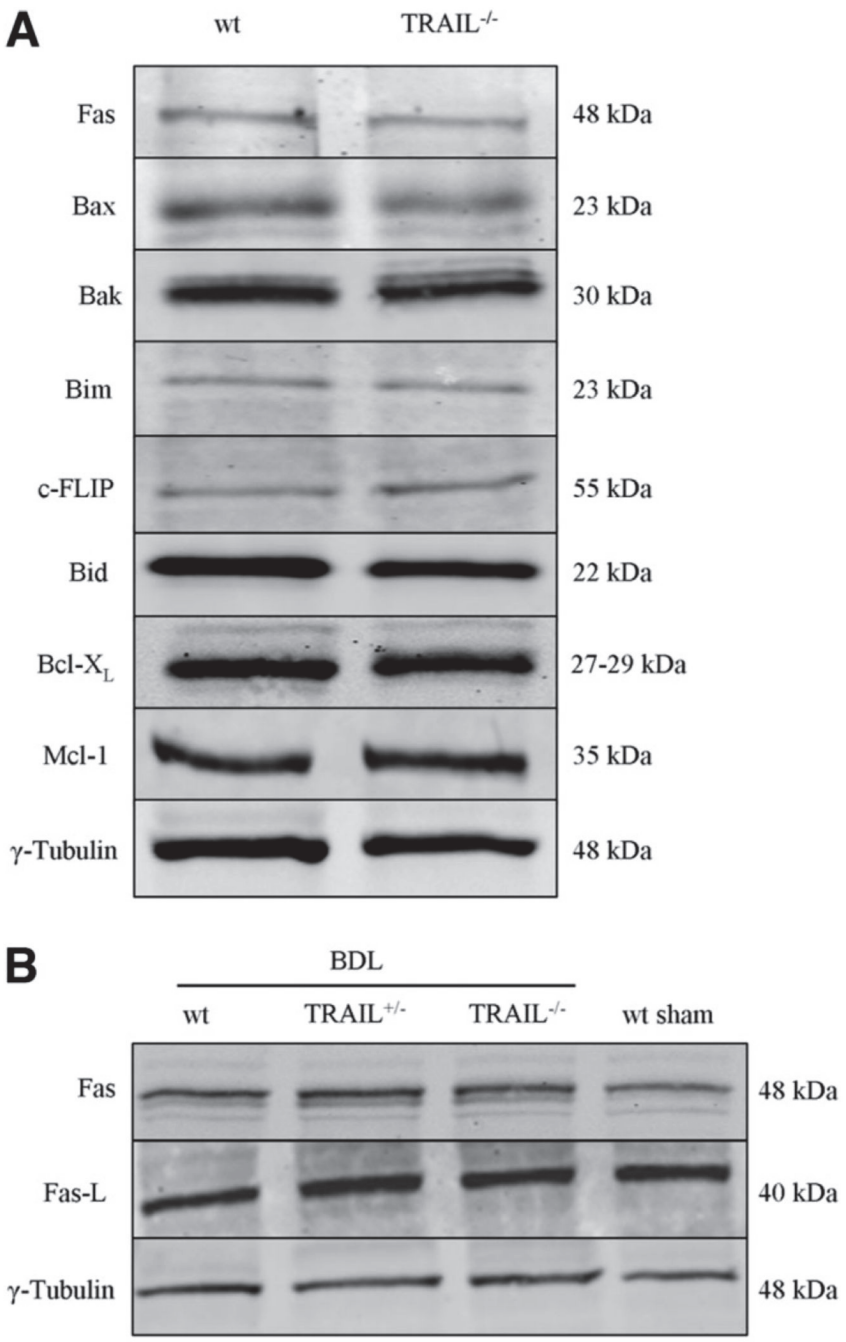

Fig. 5.

Protein expression of apoptosis effectors is similar between the different mouse genotypes. Aliquots of 50 μg of hepatic protein were subjected to SDS-PAGE and western blot analyses. The depicted blots are representative of five separate experiments, and a representative immunoblot from each animal group is shown. (A) Western blot analyses were performed for several apoptosis-related proteins in wt and TRAIL$^{-/-}$ animals under basal conditions. γ-Tubulin was used as the control for protein loading. (B) No alterations in the expression levels of the Fas receptor and ligand were observed in wt, TRAIL$^{+/-}$, and TRAIL$^{-/-}$ mice following BDL.

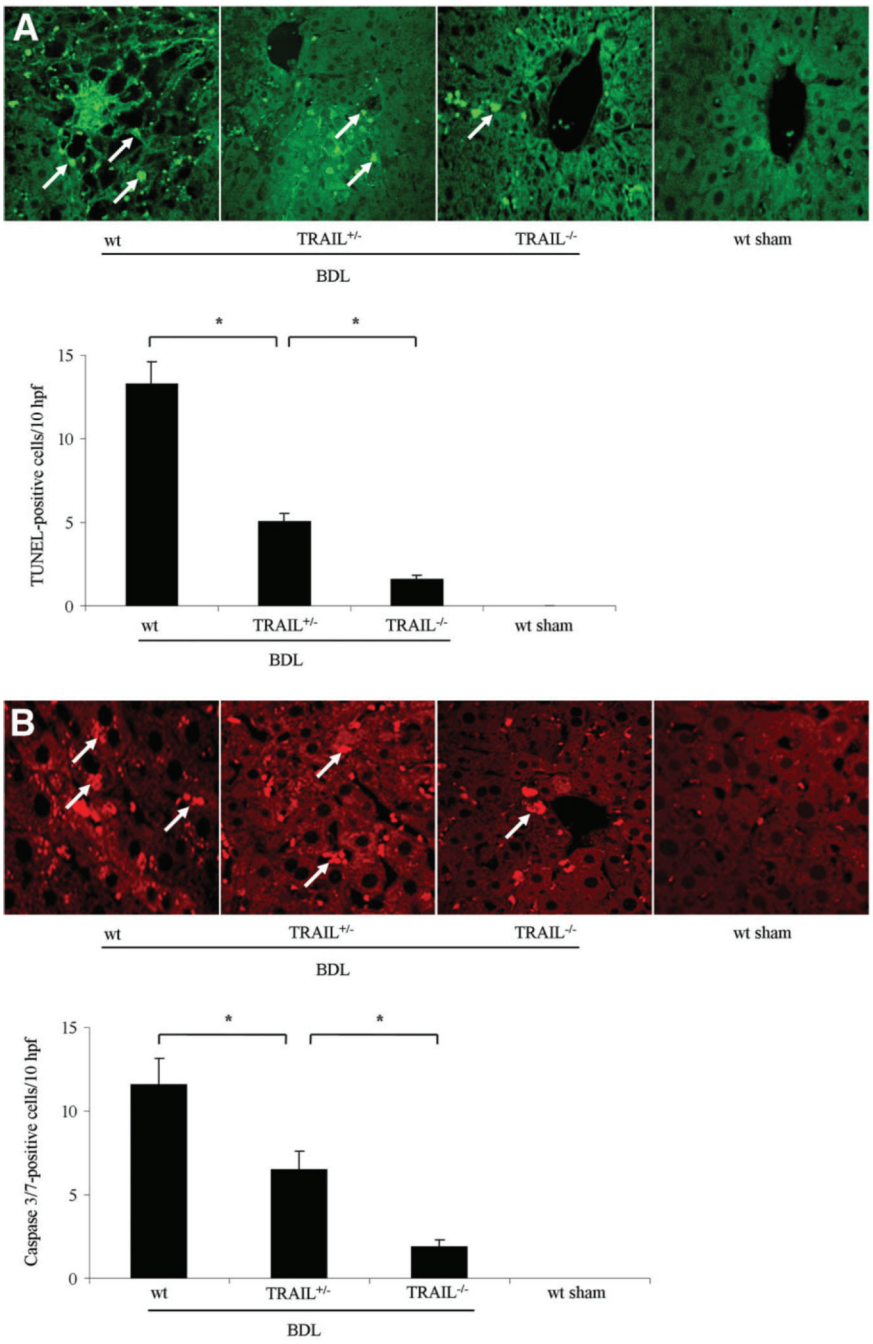

Fig. 6.

Hepatocyte apoptosis is reduced in TRAIL$^{-/-}$ mice following BDL. (A) The number of TUNEL-positive cells (marked with arrows) was quantitated and expressed as apoptotic cells/10 high-power fields (hpf). Data are from five independent animals per group and are expressed as the mean ± standard error. *$P < 0.05$ by ANOVA for wt mice versus TRAIL$^{-/-}$ mice following BDL. (B) Immunohistochemistry for the neo-epitopes of caspases 3/7 was performed (arrows indicate caspase 3/7–positive cells). Data points represent experiments from five independent animals, and bars are expressed as the mean ± standard error. *$P < 0.05$ by ANOVA for wt mice versus TRAIL$^{-/-}$ mice following BDL.

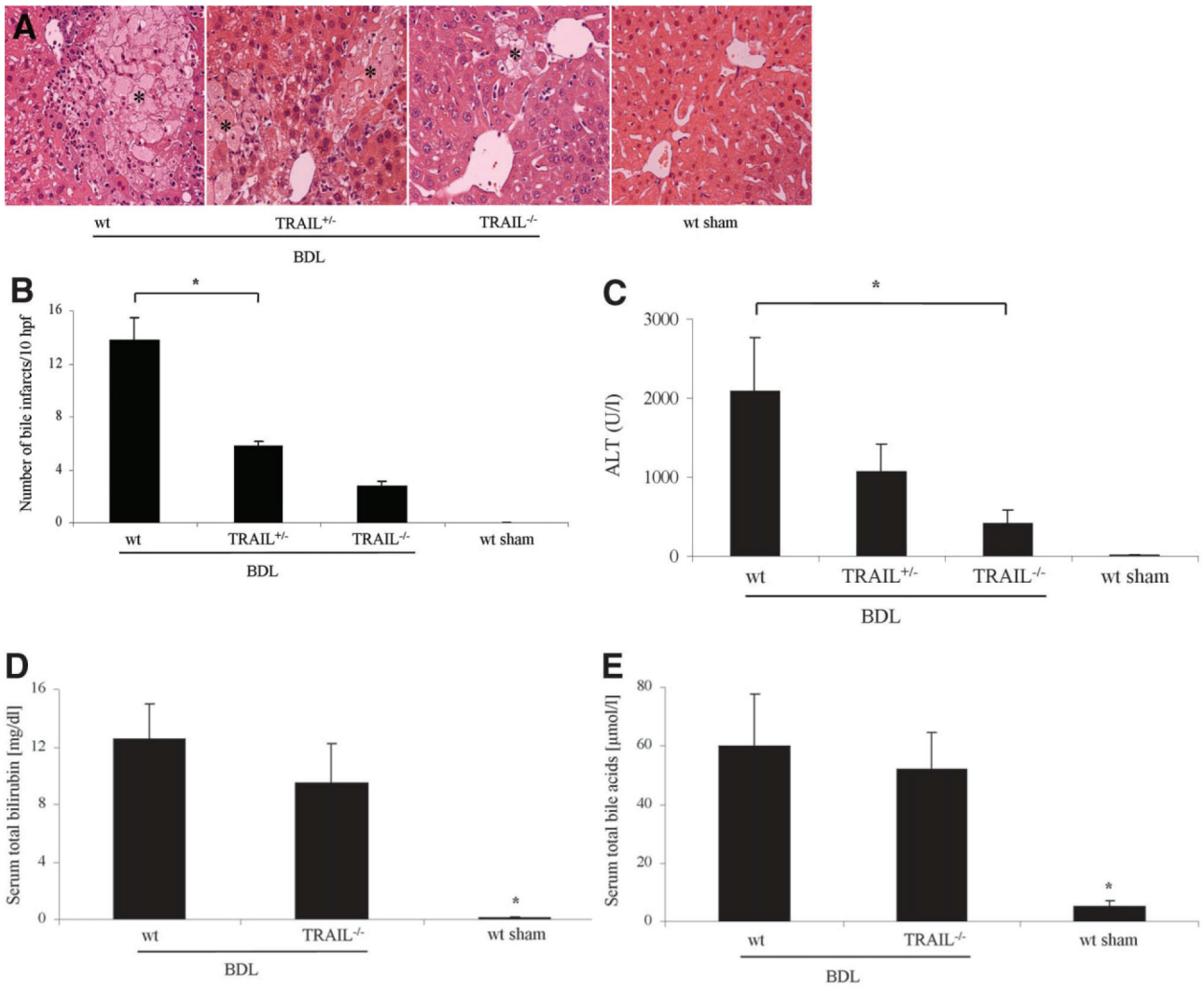

Fig. 7.

Liver injury is attenuated in TRAIL-deficient mice. wt, TRAIL$^{+/-}$, and TRAIL$^{-/-}$ mice were subjected to common BDL. On day 7 post-surgery, mice were sacrificed to obtain liver and serum samples for histological examination and determination of ALT values. (A) Representative photomicrographs of conventional H&E-stained liver sections (magnification 40X) are shown. Liver specimens of wt BDL mice displayed significant and extensive hepatocyte injury with bile infarcts (marked with asterisks). BDL-induced liver injury was reduced in TRAIL-deficient animals and was absent in liver sections of sham-operated control mice. (B) Bile infarcts were quantified in BDL wt and TRAIL-deficient mice. (C) Serum ALT values were measured 7 days after BDL. Data are from five independent animals and are expressed as the mean ± standard error. *$P < 0.05$ by ANOVA for wt mice versus TRAIL$^{-/-}$ mice following BDL. (D) Serum total bilirubin determinations were quantified 7 days after BDL. *$P < 0.01$ by ANOVA for BDL mice versus sham-operated mice. (E) Total serum bile acid concentrations were identical between BDL wt and TRAIL$^{-/-}$ animals. Data are from five independent animals and are expressed as the mean ± standard error. *$P < 0.01$ by ANOVA for BDL wt mice versus sham-operated wt mice.

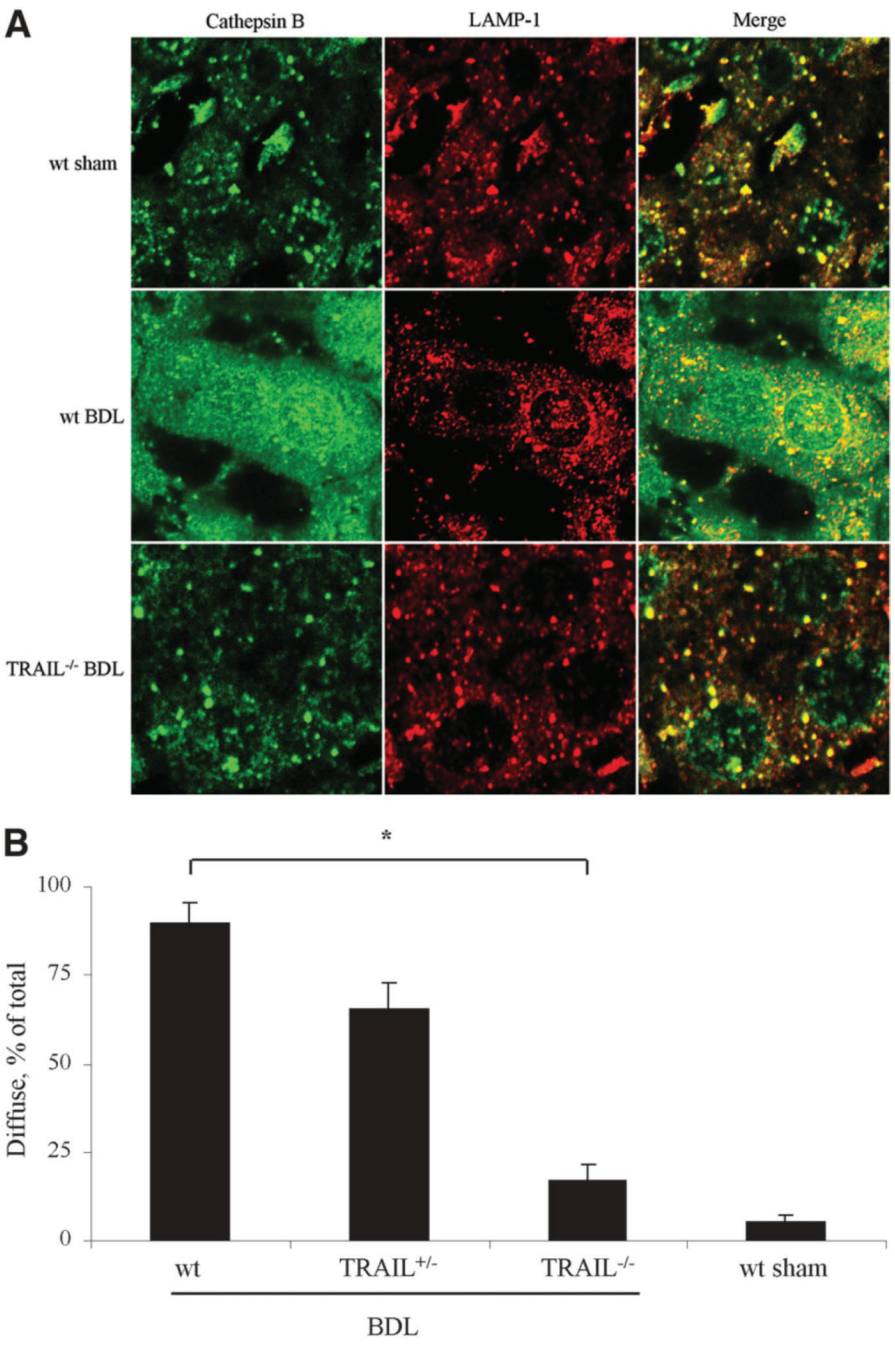

Fig. 8.

Lysosomal release of cathepsin B 7 days following BDL. (A) One week after the surgical procedure, liver tissue was obtained and analyzed by co-immunofluorescence for subcellular distribution of cathepsin B and LAMP-1. Liver tissue was viewed and imaged for punctate or diffuse appearance of the antigens by confocal microscopy using digital image analysis.(B) Quantitation of hepatocytes presenting a diffuse distribution of cathepsin B. Data are from 5 independent animals and are expressed as the mean ± standard error. *$P < 0.05$ by ANOVA.

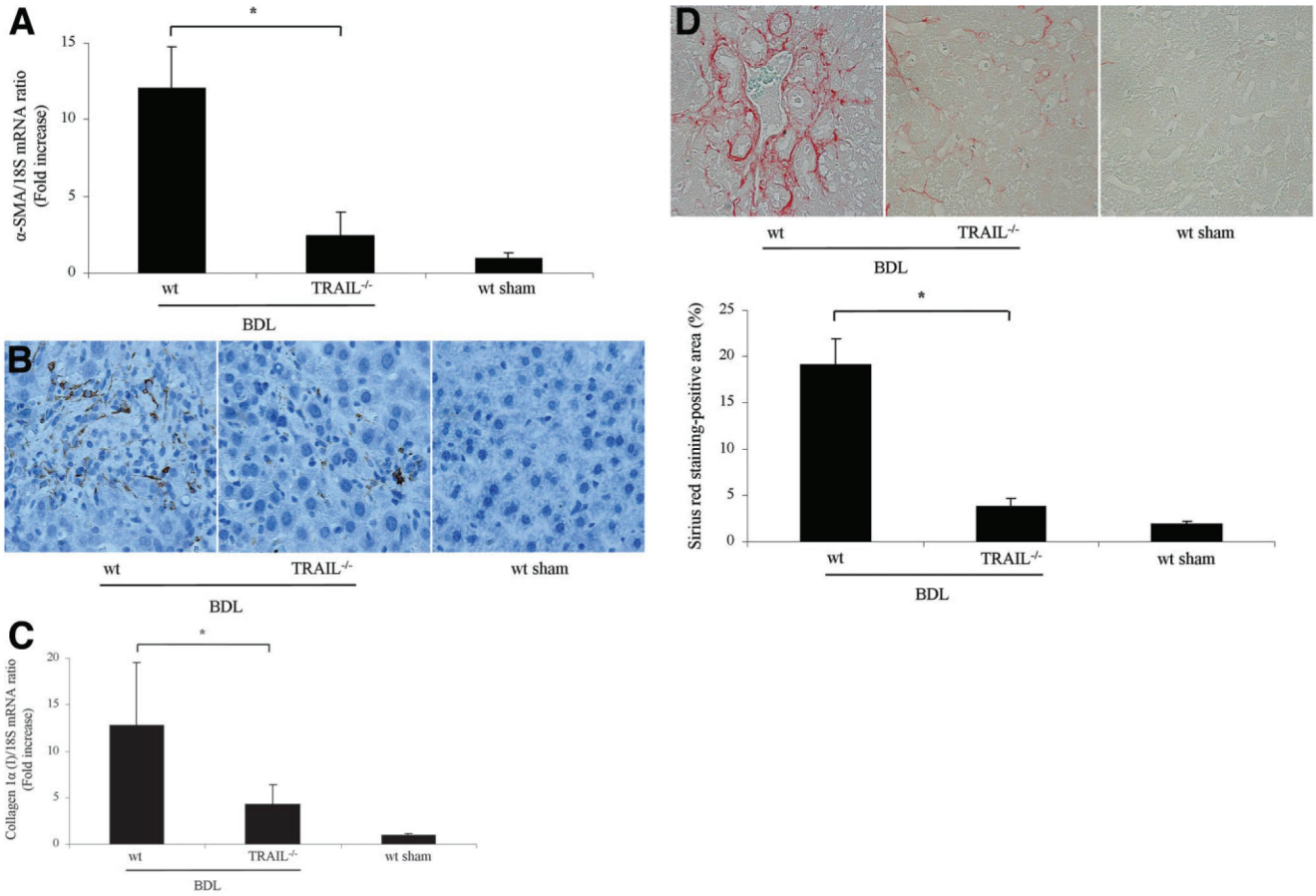

Fig. 9.

Hepatic fibrosis is reduced in TRAIL$^{-/-}$ animals following BDL. (A) Mice underwent BDL, and 14 days after the surgical procedure, liver tissue was procured to isolate total hepatic RNA. α-SMA and collagen 1α (I) mRNA expression, markers for stellate cell activation and hepatic fibrogenesis, were quantified by rt-PCR. Data were obtained from five independent animals and are expressed as the mean ± standard error. *$P < 0.05$ by ANOVA. (B) Photomicrographs after immunohistochemistry for α-SMA following BDL of 14 days are depicted. (C) Expression of collagen 1α (I) mRNA was quantified by rt-PCR 14 days after BDL (n = 5 for each group). *$P < 0.05$ by ANOVA. (D) Sirius red staining, a chemical stain of collagen deposition in the liver, was performed 14 days after BDL. Collagen fibers stained with Sirius red were quantitated using digital image analysis. Representative photomicrographs of liver sections are depicted (magnification by light microscopy 40X). Sirius red staining was quantitatively greater in wt mice than in TRAIL$^{-/-}$ mice following BDL for 14 days (n = 5 for each group). *$P < 0.05$ by ANOVA.

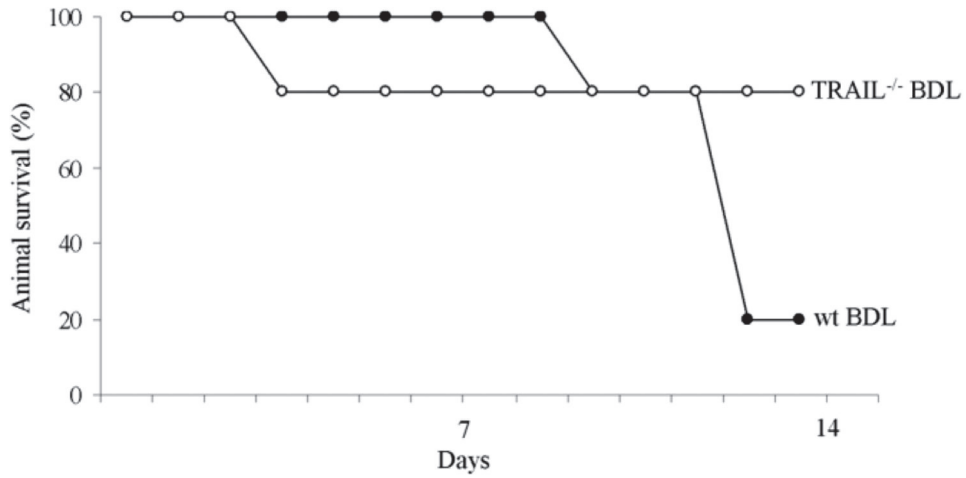

Fig. 10.

Animal survival following BDL is enhanced in TRAIL$^{-/-}$ animals. Overall animal survival is improved in BDL TRAIL$^{-/-}$ mice as compared to wt animals. Initially, on day 4 after BDL, 80% of TRAIL$^{-/-}$ animals were alive, whereas 100% of the wt mice survived cholestatic liver injury. However, on day 13 after BDL, 80% of TRAIL$^{-/-}$ animals were still alive compared to only 20% in the wt animal group.